

# Heteropolyacid@creatin-halloysite clay: an environmentally friendly, reusable and heterogeneous catalyst for the synthesis of benzopyranopyrimidines

Samahe Sadjadi<sup>1</sup>  · Majid M. Heravi<sup>2</sup> · Masoumeh Malmir<sup>2</sup>

Received: 4 April 2017 / Accepted: 19 June 2017  
© Springer Science+Business Media B.V. 2017

**Abstract** A novel hybrid catalyst has been designed and synthesized based on the incorporation of heteropolyacid into creatin-functionalized halloysite clay. The catalyst was characterized by using SEM/EDS, FTIR, XRD, BET, ICP-AES, TGA and DTGA, and successfully applied for promoting the synthesis of two series of benzopyranopyrimidines under ultrasonic irradiation in aqueous media. The results established the efficiency of this protocol in terms of product yield, reaction time and the eco-friendly nature of the process. Moreover, immobilization of heteropolyacid on creatin-functionalized halloysite circumvents heteropolyacid leaching and rendered the catalyst highly reusable.

**Keywords** Halloysite clay · Heterogeneous catalyst · Ultrasonic irradiation · Benzopyranopyrimidines · Heteropolyacids · Reusable catalyst

## Introduction

The investigation of multi-component reactions (MCRs) is a cheering and hot topic in organic chemistry. Using MCRs in the synthesis of heterocyclic molecules and drug discovery benefits from various advantageous such as high efficiency, simplicity, atom economic nature and short reaction times [1]. Fused pyrimidines

---

✉ Samahe Sadjadi  
samahesadjadi@yahoo.com

✉ Majid M. Heravi  
mmh1331@yahoo.com

<sup>1</sup> Gas Conversion Department, Faculty of Petrochemicals, Iran Polymer and Petrochemical Institute, PO Box 14975-112, Tehran, Iran

<sup>2</sup> Department of Chemistry, School of Science, Alzahra University, PO Box 1993891176, Vanak, Tehran, Iran

and benzopyranopyrimidines are biologically attractive heterocycles with pharmacological activity [2]. Some benzopyranopyrimidines are recognized as important pharmacophores that display *in vivo* antitumor activity and cytotoxic activity against cancer cell lines [3]. Owing to the wide applications of benzopyranopyrimidines, the development of new approaches for the synthesis of these valuable scaffolds is an attractive topic of current research in many laboratories [4–7]. Although various protocols have been reported for the synthesis of this class of heterocycles, very many of them suffer from some drawbacks such as high temperature, long reaction times, low yields and the use of toxic organic solvents, reagents and catalysts. Therefore, the development of new strategies and the exploitation of eco-friendly and heterogeneous catalysts to cleanly and quickly build this type of heterocyclic compounds is imperative.

Heteropolyacids (HPAs) and their salts are nontoxic catalytic species which consist of cations and polyanion clusters. These catalysts have received increasing attention due to their outstanding features such as high thermal stability, non-corrosive entity, and sensitivity to electricity and light [8]. Of note, HPAs can be considered as bifunctional catalysts which possess both strong Bronsted acidity and redox potentiality. HPAs can not only be used as classic catalysts for promoting various organic transformations [9], such as Friedel–Crafts acylation and alkylation [10], ring opening reactions, etc. [11], but have also proved to be promising photocatalysts [12] for the degradation of hazardous chemicals and electro-catalysts [13]. Moreover, HPAs have been widely used for developing hybrid catalytic systems. Despite all the excellent properties of HPAs, their solubility in water and most organic solvents, as well as their low surface area, renders them homogeneous and hampers their recovery and reuse, thus restricting their industrial applications. To furnish a solution to these drawbacks, HPAs can be immobilized on heterogeneous supports such as clays [14, 15].

Halloysite nanotubes (HNTs), a hydrated layered aluminosilicate of the kaolinite group, can be found in nature and possess the general formula of  $(\text{Al}_2(\text{OH})_4\text{Si}_2\text{O}_5 \cdot 2\text{H}_2\text{O})$  [16, 17]. The length of HNTs range from about 100 nm to 4000 nm, with an average of about 1200 nm [18]. The compositions of the interior and exterior surfaces of HNTs are different. The Al–OH octahedral sheets are located in the HNTs' inner surface, whereas the siloxanes are placed in the external surface. A monolayer of water molecules separates the unit layers of HNTs. This class of clays has gained particular interest in various research fields, such as catalysis [19, 20], materials science, drug delivery [20], photo-degradation [17], water treatment [21], optical, magnetic and electrical applications [20], membranes for gas separation [22] and enzyme immobilization, due to their properties such as biocompatibility, high surface area, availability, mechanical strength, capacity of cation exchange and porous structure. Another interesting feature of HNTs is their capability of functionalization of their both surfaces [23] and the incorporation of various active species such as nanoparticles [24, 25].

In continuation of our efforts [26–32] for developing efficient heterogeneous catalysts for promoting organic transformations, heterogenation of HPA via its immobilization on creatin-functionalized HNTs is reported here. The catalytic activity of the obtained catalyst, HPA@HNTs-C, was studied for the synthesis of

two series of benzopyranopyrimidines from the reaction of aldehydes, urea/thiourea and 4-hydroxycoumarin (method a) and the reaction of 2-hydroxy benzaldehydes, malononitrile and amine (method b). The reactions were performed under eco-friendly reaction conditions, i.e. ultrasonic irradiation in aqueous media.

## Experimental

### Chemicals and apparatus

All chemicals, including halloysite nanoclay, (3-chloropropyl) trimethoxysilan, creatin, phosphomolybdic acid, 4-hydroxy coumarine, malononitrile, aldehydes, amines, urea, thiourea, toluene, acetonitrile, and ethanol, were purchased from Sigma Aldrich and used without further purification. The synthesized catalyst was characterized by various techniques including FTIR, SEM/EDX, TGA, DTGA, XRD and ICP-AES. FTIR spectra were obtained by using a Perkin-Elmer Spectrum 65 instrument. SEM/EDS images as well as elemental mapping were recorded by employing a Tescan instrument, using Au-coated samples and an acceleration voltage of 20 kV. Room-temperature powder X-ray diffraction patterns were collected using a Siemens D5000.  $\text{CuK}\alpha$  radiation was used from a sealed tube. The BET analyses were performed using a Belsorp Mini II instrument. Prior to BET analyses, the samples were degassed at 423 K for 3 h. All the synthesized heterocycles were known and identified by comparing their melting points (measured by using the capillary tube method with an electrothermal 9200 apparatus) and FTIR spectra with authentic samples. For some samples,  $^{13}\text{C}$ NMR and  $^1\text{H}$ NMR were also obtained to prove the formation of the final products.

### Cl-Functionalization of HNTs: synthesis of HNTs-Cl

To introduce Cl functionality on HNTs, 1.2 g HNTs was added to a solution of 4 mL (3-chloropropyl) trimethoxysilan in 50 mL dry toluene. The resulting mixture was subjected to ultrasonic irradiation at 200 W for 0.5 h and then refluxed at 110 °C for 24 h. Upon completion of the process, the precipitate was filtered off and washed repeatedly with dried toluene and dried at 100 °C overnight.

### Conjugation of creatin to HNTs-Cl: synthesis of HNTs-C

To a suspension of HNTs-Cl (1 g) in 60 mL of dried toluene, creatin (0.5 g) was added. The obtained mixture was then refluxed overnight. At the end of the reaction, the solid was filtered, washed with dry toluene (20 mL) for several times and dried at 100 °C in an oven overnight.

### Immobilization of HPA on HNTs-C: synthesis of HPA@HNTs-C

Incorporation of phosphomolybdic acid on HNTs-C was achieved via the incipient wetness impregnation method. Typically, a solution of  $\text{H}_3\text{PMo}_{12}\text{O}_{40}$  20% w/w

(0.2 g of HPA in 10 mL of acetonitrile) was dropwise added to a suspension of the HNTs-C (1 g) in acetonitrile (25 mL). The resulting mixture was stirred vigorously at room temperature overnight. Subsequently, the obtained precipitate was filtered, washed with acetonitrile (20 mL) and dried in an oven at 90 °C overnight. The schematic synthesis of the catalyst is depicted in Scheme 1.

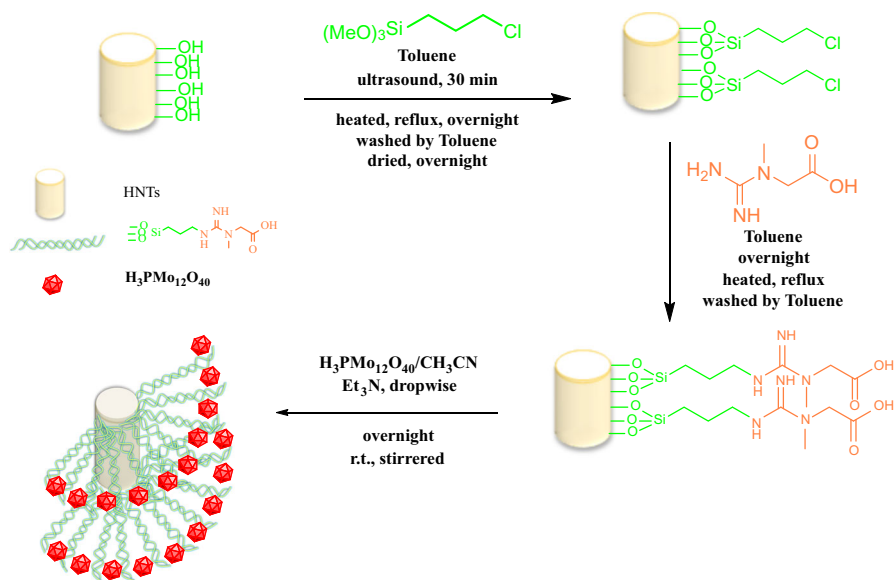
## Synthesis of benzopyranopyrimidines via two methods of a and b

### Method a

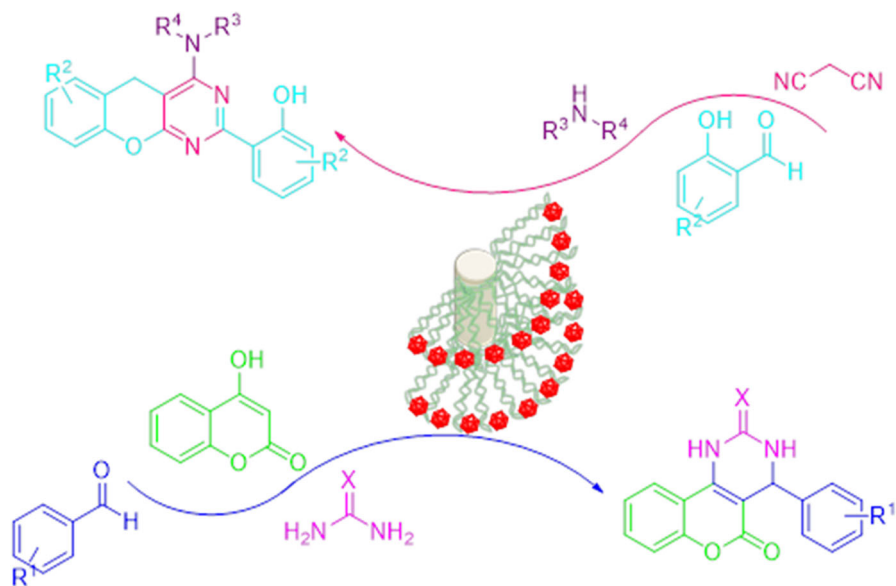
A mixture of aldehydes (1 mmol), urea/thiourea (1 mmol), 4-hydroxycoumarin (1 mmol) and catalyst (0.03 g) in 10 mL water was subjected to ultrasonic irradiation at room temperature for the appropriate reaction time. Upon completion of the reaction as monitored by TLC, the mixture was cooled to room temperature and the solid catalyst was separated by filtration, washed with H<sub>2</sub>O/EtOH (1:1) (20 mL) and dried at 90 °C overnight for reusing in consecutive reaction runs. The white solution was recrystallized from hot EtOH to afford the pure product.

### Method b

Another series of benzopyranopyrimidines was also synthesized from the reaction of 2-hydroxybenzaldehydes (2 mmol), malononitrile (1 mmol) and amines (1 mmol) in the presence of the catalyst (0.03 g) through a procedure similar to method a (Scheme 2).



**Scheme 1** Synthesis of HPA@HNTs-C as catalyst



**Scheme 2** Synthesis of benzopyranopyrimidine by two different methods a (blue line) and b (pink line). (Color figure online)

### Spectral data from some of the compounds

#### *3,4-Dihydro-4-phenyl-1H-chromeno [4,3-d] pyrimidine-2,5-dione (4a)*

White solid, m.p. 160–162 °C; IR: (KBr) ( $\nu$   $\text{cm}^{-1}$ ) = 3409, 2920, 2730, 2365, 1648, 1450, 1354, 1300, 1120, 1068, 972, 722; <sup>1</sup>H-NMR (DMSO):  $\delta$ (ppm) 6.35 (s, 1H, CH), 7.10–7.55 (m, 9H, Ar-H), 7.75 (brs, 1H, NH), 7.85 (brs, 1H, NH).

#### *4-(4-Chlorophenyl)-3,4-dihydro-1H-chromeno [4, 3-d] pyrimidine-2, 5-dione (4b)*

White solid, m.p. 162–164 °C; IR: (KBr) ( $\nu$   $\text{cm}^{-1}$ ) = 3400, 3075, 2888, 2825, 2730, 2610, 1659, 1604, 1556, 1490, 1446, 1343, 1309, 1217, 1086, 1034, 1010, 760, 671; <sup>1</sup>H-NMR (DMSO):  $\delta$ (ppm) 6.34 (s, 1H, CH), 7.28–7.66 (m, 8H, ArH), 7.89 (brs, 1H, NH), 7.95 (brs, 1H, NH).

#### *1,2,3,4-Tetrahydro-4-(2-hydroxyphenyl)-2-thioxochromeno[4, 3-d]pyrimidin-5-one (4g)*

Pale yellow, m.p. 169–171 °C; IR: (KBr) ( $\nu$   $\text{cm}^{-1}$ ) = 3413, 3067, 2360, 1748, 1600, 1475, 1441, 1380, 1336, 1240, 1262, 1021, 940, 870, 760, 465. <sup>1</sup>H-NMR (300 MHz, DMSO):  $\delta$ (ppm) 3.35 (brs, 1H, OH), 6.9–7.76 (m, 9H, Ar-H), 8.40 (brs, 1H, NH), 10.75 (brs, 1H, NH).

*2-(4-Morpholino-5H-chromeno[2,3-d]pyrimidin-2-yl)phenol (8a)*

White powder, m.p. 160–162 °C; IR: (KBr) ( $\nu$   $\text{cm}^{-1}$ ) = 3449, 3098, 2990, 1605.  $^1\text{H-NMR}$  (400 MHz,  $\text{CDCl}_3$ ):  $\delta$  (ppm) 3.51 (t,  $J = 4.5$  Hz, 4H), 3.89 (t,  $J = 4.5$  Hz, 4H), 3.90 (s, 2H), 6.96 (t,  $J = 8.0$  Hz, 1H), 6.99 (d,  $J = 8.0$  Hz, 1H), 7.11 (t,  $J = 7.3$  Hz, 1H), 7.20–7.32 (m, 3H), 7.38 (t,  $J = 7.3$  Hz, 1H), 8.40 (d,  $J = 8.0$  Hz, 1H).  $^{13}\text{C-NMR}$  (100 MHz,  $\text{CDCl}_3$ ):  $\delta$  (ppm) 25, 48.9, 66.2, 96.6, 115.5, 115.4, 118.5, 118.7, 118.9, 124, 128, 128.2, 129.5, 133.7, 149.2, 161.2, 161.9, 163, 164.7 ppm.

*2-Methoxy-6-(9-methoxy-4-morpholino-5H-chromeno[2,3-d]pyrimidin-2-yl)phenol (8b)*

White powder, m.p. 162–164 °C; IR: (KBr) ( $\nu$   $\text{cm}^{-1}$ ) = 3444, 3043, 2950, 1600.  $^1\text{H-NMR}$  (400 MHz,  $\text{CDCl}_3$ ):  $\delta$  (ppm) 3.45 (t,  $J = 4.4$  Hz, 4H), 3.90 (t,  $J = 4.4$  Hz, 4H) 3.94 (s, 8H), 6.70 (d,  $J = 7.7$  Hz, 1H), 6.80–6.90 (m, 2H), 6.91 (d,  $J = 7.7$  Hz, 1H), 6.99 (t,  $J = 8.0$  Hz, 1H), 8.07 (d,  $J = 8.0$  Hz, 1H).  $^{13}\text{C-NMR}$  (100 MHz,  $\text{CDCl}_3$ ):  $\delta$  (ppm) 25.1, 48.7, 55.9, 55.91, 66.43, 97.6, 111.5, 113.5, 118, 118.4, 119.6, 119.9, 121, 124.5, 139.7, 148, 148.5, 150.9, 162.5, 165.3.

*2-Methoxy-6-(9-methoxy-4-(piperidin-1-yl)-5H-benzopyran[2,3-d]pyrimidin-2-yl)phenol (8e)*

White powder, m.p. 181–183 °C; IR: (KBr) ( $\nu$   $\text{cm}^{-1}$ ) = 3415, 3044, 2926, 1604;  $^1\text{H-NMR}$  (400 MHz,  $\text{CDCl}_3$ ):  $\delta$  (ppm) 1.65–1.81 (m, 6H), 3.45 (t,  $J = 4.9$  Hz, 4H), 3.76 (s, 2H), 3.95 (s, 6H), 6.80 (d,  $J = 7.7$  Hz, 1H), 6.85–6.91 (m, 2H), 6.95 (d,  $J = 7.7$  Hz, 1H), 7.06 (t,  $J = 8.0$  Hz, 1H), 8.12 (d,  $J = 8.0$  Hz, 1H).  $^{13}\text{C-NMR}$  (100 MHz,  $\text{CDCl}_3$ ):  $\delta$  (ppm) 24.5, 25.6, 27.7, 50.3, 55.7, 55.9, 99.6, 110.1, 114.7, 118.2, 118.5, 120.1, 120.2, 120.8, 124, 138.9, 146.7, 149, 150.2, 162.3, 165.1, 166.4.

## Results and discussion

### Characterizations of catalyst

The SEM/EDX images of the HPA@HNTs-C are depicted in Fig. 1. As can be seen, upon functionalization of the HNTs with creatin and incorporation of HPA, the morphology of the HNTs changed to a more aggregate one. According to previous reports [19], this observation can be attributed to the presence of organic functionalities which can anchor the HPA and keep the HNTs nano-rods more packed. Notably, in the SEM images of the HPA@HNTs-C, the rod-like morphology is still observable, indicating that upon functionalization the tubular morphology of the HNTs did not collapse. This observation was also confirmed via XRD analysis. The EDX analysis of the catalyst established the presence of Si, Al and O atoms which can be attributed to the HNTs framework. Moreover, the C, O

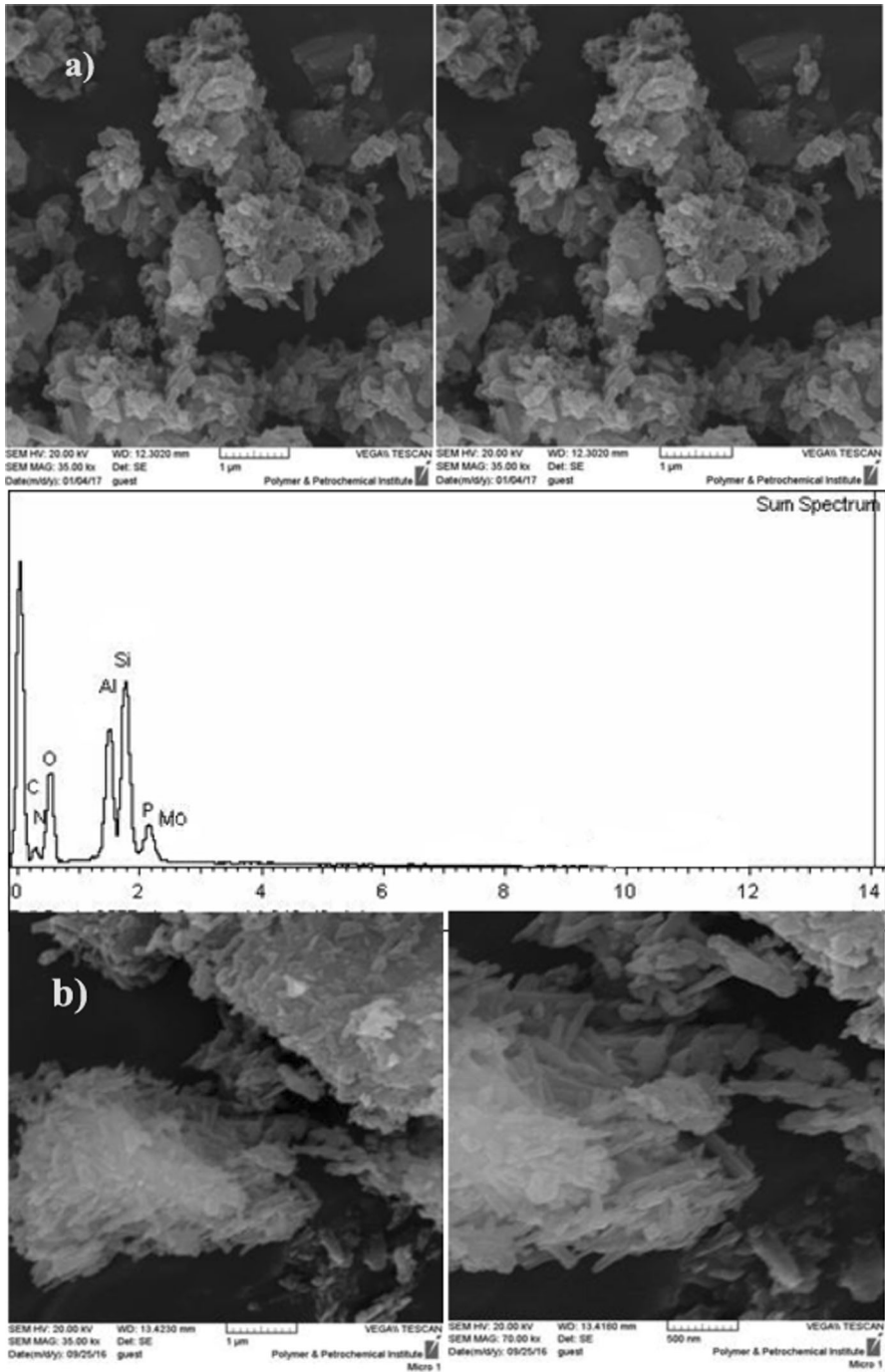


Fig. 1 The SEM/EDX images of HPA@HNTs-C (a) and SEM image of pure HNTs (b) [11, 19]

and N atoms can demonstrate the successful conjugation of creatin to the HNTs. The Mo and P atoms represent the presence of HPA in the structure of the final catalyst.

The FTIR spectrum of the catalyst is illustrated in Fig. 2. The spectrum contains the characteristic bands of HNTs, i.e. 3705 and 3631  $\text{cm}^{-1}$ , which can be assigned to internal and external hydroxyl groups of HNT. According to the literature, the deformation vibration of Al–O–Si at 528  $\text{cm}^{-1}$  is due to Al–O tetrahedral sheets and the Si–O–Si deformation vibration at 458  $\text{cm}^{-1}$  can be assigned to Si–O tetrahedral sheets [33].

The bands at 3093 and 1047  $\text{cm}^{-1}$ , which are representative of  $-\text{CH}_2$  stretching and Si–O stretching, can prove the successful attachment of (3-chloropropyl)trimethoxysilan. The bands at 1679, 1699 and 3274  $\text{cm}^{-1}$ , which are due to the stretching vibration of C = N, C = O and  $-\text{NH}_2$ , establish the presence of creatin in the structure of the catalyst. Moreover, the bands at 1047, 810, 609, and 916  $\text{cm}^{-1}$  can be assigned to the symmetric stretching of P–O, Mo–Oc–Mo, Mo–Oe–Mo and Mo–Ot, respectively, and prove the HPA incorporation [34]. The FTIR spectrum of the catalyst is distinguished from the pure HNTs [35], in which no characteristic band can be observed for C = N, C = O,  $-\text{CH}_2$  stretching.

The XRD pattern of the catalyst and pure HNTs are shown in Fig. 3. The reflections observed at 7.53°, 13.74°, 23.44°, 28.78°, 32.48°, 58.94° and 67.18° can be assigned to HNTs (JCPDS No. 29-1487). This pattern is in good accordance with the XRD patterns, reported for HNTs in the literature [36, 37]. Comparing these two XRD patterns clearly establishes their similarity. This observation indicated that, upon HNTs functionalization and HPA incorporation, the tubular structure of HNTs did not collapse. Notably, the interlayer distance of the HPA@HNTs-C remained unchanged compared to pure HNTs, implying that the incorporation of the creatin and HPA did not take place between the interlayer of the HNTs. This result is in good accordance with previous reports [37]. All the observed peaks can be assigned to HNTs and no distinguished peak was detected for the HPA. According to the

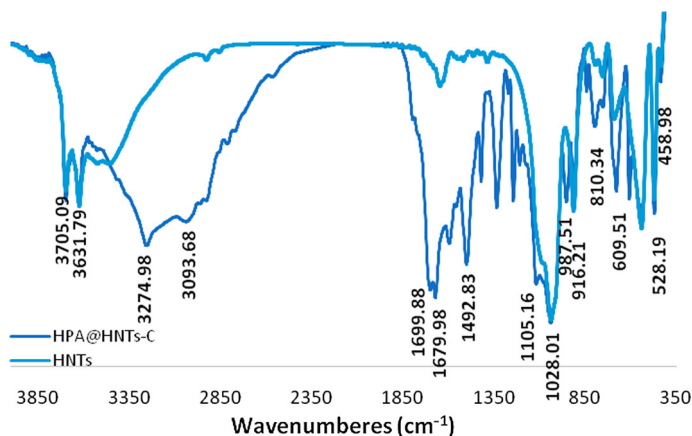


**Fig. 2** FTIR spectra of pure HNTs and HPA@HNTs-C [26, 35]

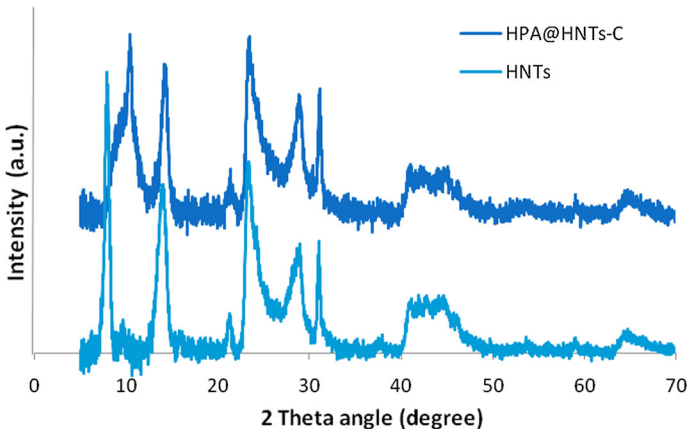


**Fig. 3** XRD pattern of pure HNTs and HPA@HNTs-C

previous reports, this can be due to the low amount of HPA as well as its high dispersion on the functionalized HNTs [34].

To provide more insight into the catalyst structure, DTGA and TGA thermograms of the catalyst were obtained (Fig. 4). As shown, two degradation stages can be detected over the range of 45–600 °C. The first degradation can be due to the loss of adsorbed water molecules. The other observed weight losses (at about 480 °C) can be assigned to the thermal decomposition of other components. Notably, the TGA thermogram of the HPA@HNTs-C is totally distinguished from pure HNTs [38, 39], in which one degradation step occurred in the range of 45–600 °C due to loss of lattice water. TGA analysis was also exploited for calculating the content of the organic motif of the catalyst. This value was about 16 w/w%.

To calculate the content of HPA in the final catalyst, the HPA was digested in concentrated hydrochloric and nitric acids solution. Then, the resulting extract was

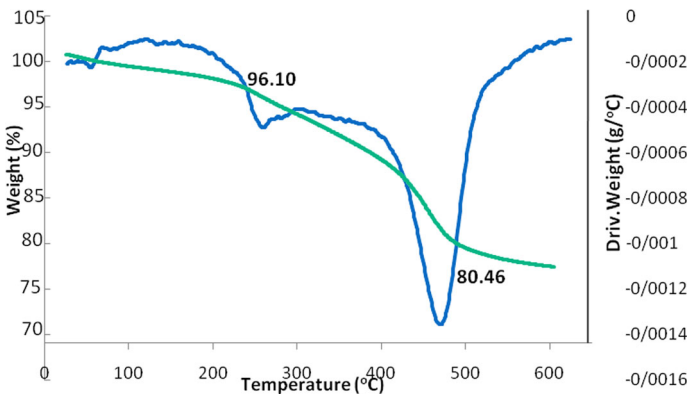


**Fig. 4** The TGA (a) and DTGA (b) analysis of HPA@HNTs-C

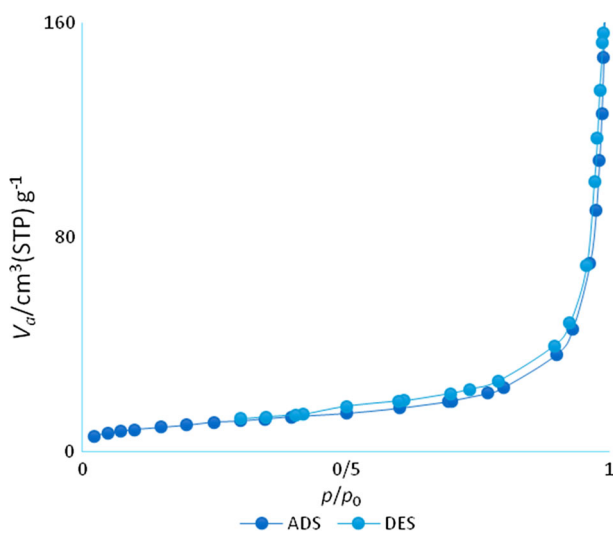
analyzed using ICP-AES. The result showed that the loading of HPA was about 6 w%.

A nitrogen adsorption–desorption isotherm of the final catalyst was also recorded to investigate the textural properties of HPA@HNTs-C (Fig. 5). The shape of the isotherm is indicative of the type II nitrogen adsorption–desorption isotherms with H3 hysteresis loops [37], and demonstrated that HPA@HNTs-C possesses the porous structure. To elucidate whether the HNTs functionalization and incorporation of HPA affect the textural properties of the pure HNTs, the average pore diameter, specific surface area and total pore volume of the HNTs and HPA@HNTs-C were compared (Table 1). The results indicate that incorporation of creatin and HPA reduced the specific surface area and pore volume while increasing the average pore diameter. This observation can imply that functionalization and immobilization of HPA can occur both on the surface and within the cavity of the HNTs.

### Catalytic activity of HPA@HNTs-C catalyst for the synthesis of benzopyranopyrimidines

To investigate the catalytic activity of the catalyst, the synthesis of two series of benzopyranopyrimidines (Schemes 3, 4) which are biologically attractive were selected as model organic transformations.

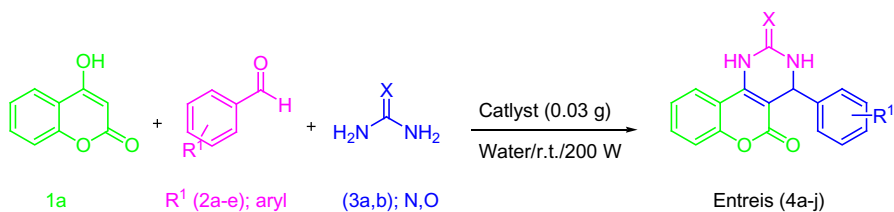
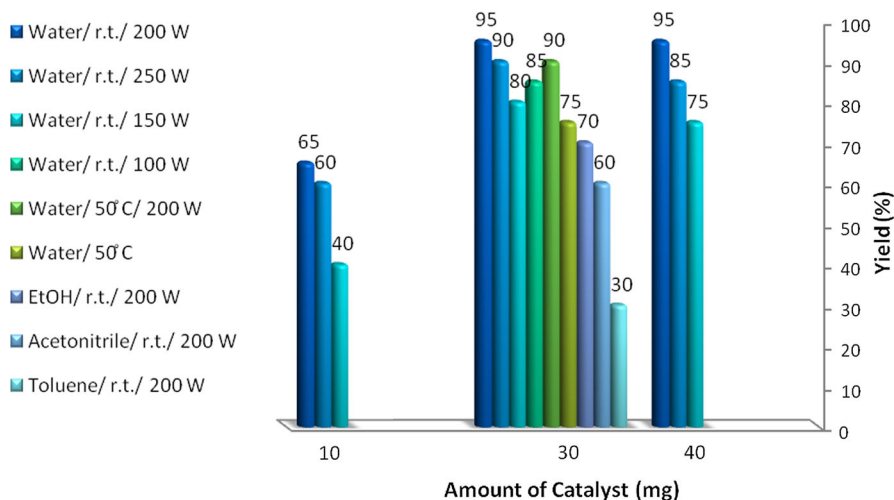
Initially, the reaction of 4-hydroxycumarine, benzaldehyde and urea and the reaction of 2-hydroxybenzaldehyde, morpholine and malononitrile were selected as the model reactions and performed in the absence of the catalyst. The results established that the presence of the catalyst was essential for promoting the reaction (Figs. 5, 6). Subsequently, the model reactions were performed in the presence of a



**Fig. 5** Nitrogen adsorption–desorption isotherms of HPA@HNTs-C

**Table 1** The BET surface area of the catalyst and pure HNTs

Sample	S <sub>BET</sub> (m <sup>2</sup> g <sup>-1</sup> )	Total pore volume (cm <sup>3</sup> g <sup>-1</sup> )	Average pore diameter (nm)
HPA@HNTs-C	16.5	0.11	27.29
HNTs	51	0.19	15.23

**Scheme 3** Synthesis of benzopyranopyrimidines using 4-hydroxycoumarin under ultrasonic irradiation**Scheme 4** Synthesis of benzopyranopyrimidines using salicylaldehydes under ultrasonic irradiation**Fig. 6** Effects of loading of catalyst, duration of reaction and solvent on the yield of benzopyranopyrimidines prepared from reaction of 4-hydroxycoumarin (1 equiv.), benzaldehyde (1 equiv.) and urea (1 equiv.)

catalytic amount (0.01 g) of the catalyst in aqueous media under ultrasonic irradiation. Gratifyingly, the desired products were obtained under eco-friendly conditions after relatively short reaction times (Figs. 6, 7).

Motivated by these results, the reaction variables, the solvent, the amount of the catalyst and the power of the ultrasonic, were optimized (Figs. 6, 7). The highest yields were obtained by using the power of 200 W in the presence of 0.03 g catalyst in water.

Armed with the optimum reaction variables, two series of benzopyranopyrimidines were synthesized by using various aldehydes and amines to demonstrate the generality of the protocols. Moreover, the thio-functionlized derivatives were achieved by replacing urea with thiourea.

As is clear, aldehydes with electron-withdrawing and electron-donating groups could be successfully used in method a (Table 2) to furnish the desired products in high yields and in very short reaction times. Of note, both urea and thiourea resulted in products in competitive yields. Regarding method b (Table 3), 2-hydroxybenzaldehydes with different electron densities could be applied. However, 2-hydroxybenzaldehyde with electron-withdrawing groups led to corresponding products with slightly lower yields.

Based on the literature [7], the suggested mechanism for the synthesis of benzopyranopyrimidines is demonstrated in Scheme 5. In the case of method b, initially, the reaction starts via formation of a Knoevenagel adduct derived from reaction of salicylaldehyde and malononitrile to form the intermediate **I** on the acidic active surface of HPA@HNTs-C. Then, the cyano group of intermediate **I** is attacked by the cyclic secondary amine to produce intermediate **II**. Finally, intermediate **II** reacts with another molecule of salicylic aldehyde involving rapid hydrogen ion transfers **III** to furnish benzopyrano[2,3-d]pyrimidine **IV**. Regarding

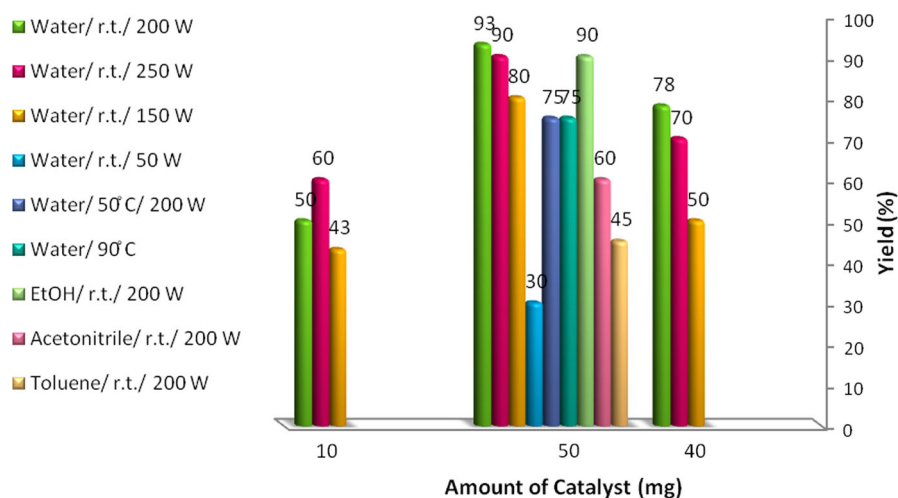


**Fig. 7** Effects of loading of catalyst, duration of reaction and solvent on the yield of benzopyranopyrimidines prepared from reaction of 2-hydroxybenzaldehyde **5a** (2 equiv.), morpholine **6a** (1 equiv.) and malononitrile (**7**) (1 equiv.)

**Table 2** Preparation of benzopyranopyrimidines (**4a–j**) from reaction of 4-hydroxycumarine, aldehyde and urea/thiourea catalyzed by HPA@HNTs-C<sup>a</sup> [4, 40]

Entry	R <sup>1</sup>	X	Time (min)	Yield (%) <sup>b</sup>	m.p. References
<b>4a</b>	<b>2a</b> :H	<b>3a</b> :O	4	95	160–162 °C (Ref. [4] 160–162 °C)
<b>4b</b>	<b>2b</b> : <i>p</i> -Cl	<b>3a</b>	13	95	162–164 °C (Ref. [31] 160–162 °C)
<b>4c</b>	<b>2c</b> : <i>m</i> -NO <sub>2</sub>	<b>3a</b>	17	85	172–174 °C (Ref. [31] 172–174 °C)
<b>4d</b>	<b>2a</b>	<b>3b</b> :S	10	85	188–190 °C (Ref. [4] 188–190 °C)
<b>4e</b>	<b>2b</b>	<b>3b</b>	15	80	188–190 °C (Ref. [31] 188–190 °C)
<b>4f</b>	<b>2c</b>	<b>3b</b>	22	90	185–187 °C (Ref. [31] 183–185 °C)
<b>4g</b>	<b>2d</b> : <i>o</i> -OH	<b>3b</b>	15	92	169–171 °C (Ref. [4] 170 °C)

<sup>a</sup> Reaction condition: a mixture of 4-hydroxycumarine **1a** (1 equiv.), aldehydes (**2a–e**; R<sup>1</sup> = aryl) (1 equiv.), urea/thiourea (**3a**, **b**) (1 equiv.) and HPA@HNTs-C (0.03 g) was reacted by ultrasonic irradiation (Method A)

<sup>b</sup> Isolated yield

**Table 3** Preparation of benzopyranopyrimidines (**8a–h**) from reaction of 2-hydroxybenzaldehyde, amines and malononitrile catalyzed by HPA@HNTs-C<sup>a</sup> [5, 41]

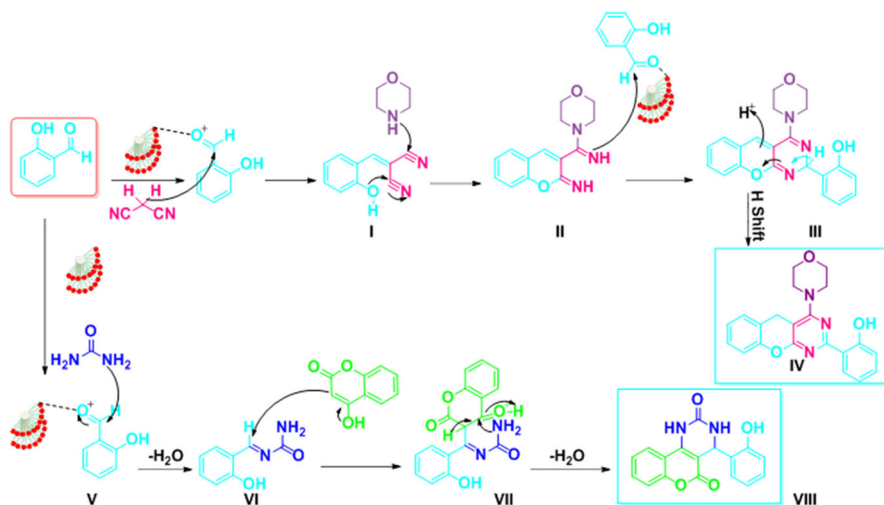
Entry	R <sup>2</sup>	R <sup>3</sup> , R <sup>4</sup>	Time (min)	Yield (%) <sup>b</sup>	m.p. References
<b>8a</b>	<b>5a</b> :H	<b>6a</b> :-(CH <sub>2</sub> ) <sub>2</sub> -O-(CH <sub>2</sub> ) <sub>2</sub> -	40	95	160–162 °C (Ref. [5] 160–162 °C)
<b>8b</b>	<b>5b</b> :3-MeO	<b>6a</b>	30	90	162–164 °C (Ref. [5] 160–162 °C)
<b>8c</b>	<b>5c</b> :5-Br	<b>6a</b>	70	80	198–200 °C (Ref. [29] 198–200 °C)
<b>8d</b>	<b>5a</b>	<b>6b</b> :-(CH <sub>2</sub> ) <sub>5</sub> -	60	85	178–180 °C (Ref. [5] 178–180 °C)
<b>8e</b>	<b>5b</b>	<b>6b</b>	50	83	181–183 °C (Ref. [5] 180–182 °C)
<b>8f</b>	<b>5c</b>	<b>6b</b>	70	78	187–189 °C (Ref. [29] 188–190 °C)
<b>8g</b>	<b>5a</b>	<b>6c</b> :CH <sub>3</sub> , CH <sub>3</sub>	60	92	178–180 °C (Ref. [5] 178–190 °C)
<b>8h</b>	<b>5b</b>	<b>6c</b>	40	80	200–202 °C (Ref. [5] 200–202 °C)

<sup>a</sup> Reaction condition: a mixture of 2-hydroxybenzaldehydes **5a** (2 equiv.), amines **6a** (1 equiv.), malononitrile **7** (1 equiv.) and HPA@HNTs-C (0.03 g) was reacted by ultrasonic irradiation (Method A) and heated (Method B) at 90 °C

<sup>b</sup> Isolated yield

method a, based on the literature [4], it is believed that the salicylic aldehyde can be activated by the catalyst (**V**). Subsequently, the reaction proceeds via a Knoevenagel condensation to produce intermediate **VI**. Then, the latter tolerated the Michael addition with 4-hydroxycumarine to generate intermediate **VII**. Finally, cyclization of **VII** gives product **VIII**, after dehydration.

In order to demonstrate the efficiency of our protocol, the yields of two model benzopyrano[2,3-*d*]pyrimidinesins (procedures a and b) under HPA@HNTs-C catalysis was compared with those of previously reported procedures and catalysts (Table 4). As shown in this table, the efficiency of HPA@HNTs-C in procedure b is superior to silica-bonded *N*-propylpiperazine sodium *N*-propionat, ZrOCl<sub>2</sub>·8H<sub>2</sub>O



**Scheme 5** A plausible mechanism of synthesis of benzopyranopyrimidine in the presence of HPA@HNTs-C

and  $\text{Na}_2\text{MoO}_4 \cdot 2\text{H}_2\text{O}$ . Moreover, compared to conventional thermal methods, this catalyst could furnish the desired product in a shorter reaction time and more eco-friendly procedure. Regarding procedure a, the previously reported procedures and catalysts led to comparative yields in less than 5 min. However, HPA@HNTs-C benefits from some advantages such as being a heterogeneous, non-corrosive and non-toxic entity.

To investigate the catalyst reusability, the model reactions were performed in the presence of the fresh and reused catalysts. The comparison of the yields of the desired products (Fig. 8) established that the catalyst could be recovered and reused with only slight loss of the catalytic activity. This promising result motivated us to study the HPA leaching to disclose whether the catalysis is heterogeneous. To this purpose, a hot filtration test was used and established only a negligible loss of HPA, detected by ICP-AES. This result not only proved the heterogeneous catalysis but also confirmed the efficient immobilization of HPA on functionalized HNTs. The low leaching of the HPA can be attributed to the interaction of HPA with the heteroatoms present in creatin. It is postulated that these interactions preserved the HPA on the HNTs surface and control the HPA leaching. To elucidate whether these interactions are responsible for low leaching of HPA, HPA was immobilized on pure HNTs, HPA@HNTs, via a simple incipient wetness impregnation method (“Immobilization of HPA on HNTs-C: synthesis of HPA@HNTs-C” section). Subsequently, the content of the HPA on the catalyst was calculated by the ICP-AES method. Interestingly, the loading of the HPA on the pure HNTs was remarkably lower (1 w/w%) than that of the creatin-functionalized HNTs (6 w/w%). This result indicated the role of creatin functionality in efficient immobilization of HPA on the HNTs surface. Notably, the catalytic activity of HPA@HNTs-C was higher than HPA@HNTs which can be related to the higher content of HPA.

**Table 4** Comparison of the efficiencies of various protocols for the synthesis of benzopyrano[2,3-d]pyrimidine<sup>a,b</sup> [4–6, 41, 42]

Entry	Catalyst (amount)	Reaction conditions	Yield (%)	Time (h:min)	References
<b>1a</b>	Chlorosulfonic acid (2.5 mol%)	Ultrasonic/r.t./S.F.	96	00:05	[4]
<b>2a</b>	Hydrochloric acid (4 drops)	Microwave/EtOH	94	00:02.6	[6]
<b>3b</b>	Silica-bonded <i>N</i> -propylpiperazine sodium <i>N</i> -propionat (0.05 g)	Thermal/r.t./S.F.	86	6:00	[30]
<b>4b</b>	ZrOCl <sub>2</sub> ·8H <sub>2</sub> O (30 mol%)	Thermal/r.t./S.F.	90	15:00	[29]
<b>5b</b>	Na <sub>2</sub> MoO <sub>4</sub> ·2H <sub>2</sub> O (10 mol%)	Thermal/r.t./EtOH	90	10:00	[5]
<b>6a</b>	HPA@HNTs-C (0.03 g)	Ultrasonic/r.t./H <sub>2</sub> O	95	00:04	[This work]
<b>7b</b>	HPA@HNTs-C (0.03 g)	Ultrasonic/r.t./H <sub>2</sub> O	95	00:40	[This work]

<sup>a</sup> Reaction condition: a mixture of 4-hydroxycumarine (1 equiv.), benzaldehyde (1 equiv.), urea (1 equiv.) was reacted by ultrasonic or microwave irradiation

<sup>b</sup> Reaction condition: a mixture of 2-hydroxybenzaldehyde (2 equiv.), malonitrile (1 equiv.), morpholine (1 equiv.) was reacted by ultrasonic irradiation or heated

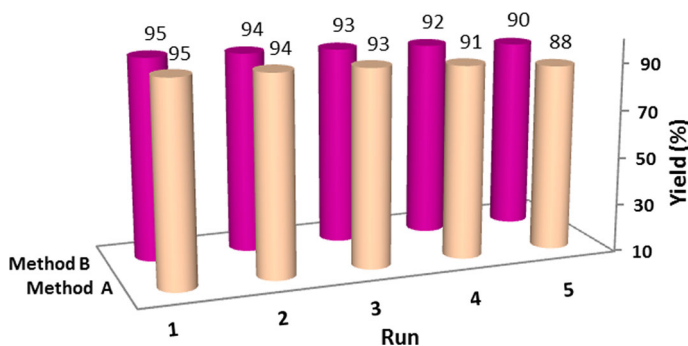


**Fig. 8** The results of studying the reusability of the catalyst for the synthesis of benzopyranopyrimidine by two different methods *a* and *b*

Moreover, studying the reusability of the HPA@HNTs established its inferior reusability compared to HPA@HNTs-C which implied the necessity of creatin for preserving HPA on the HNTs surface.

## Conclusions

In summary, a novel method for the heterogenization of HPA via immobilization on the creatin-functionalized HNTs is presented. The hybrid system was successfully applied for promoting the synthesis of biologically attractive benzopyranopyrimidines under eco-friendly ultrasonic-assisted procedure. The hot filtration method established the efficiency of this hybrid system for controlling the HPA leaching and developing a heterogeneous and reusable catalyst. Compared to the previously reported methods for the synthesis of benzopyranopyrimidines, the presented

protocol benefits from advantages such as short reaction time, high yields, excellent reusability and simplicity of the work-up procedure.

**Acknowledgements** The authors appreciate partial financial supports from Alzahra University and Iran Polymer and Petrochemical Institute. MMH is also grateful to Iran National Science Foundation for the Individual given grant.

## References

1. I. Nakamura, Y. Yamamoto, *Chem. Rev.* **104**, 2127 (2004)
2. P.G. Baraldi, M.A. Tabrizi, S. Gessi, P.A. Borea, *Chem. Rev.* **108**, 238 (2008)
3. P. Schmid, J. Krockner, C. Jehn, K. Michniewicz, S. Lehenbauer-Dehm, H. Eggemann, V. Heilmann, S. Kümmel, C.O. Schulz, A. Dieing, M.B. Wischnewsky, S. Hauptmann, D. Elling, K. Possinger, B. Flath, *Ann. Oncol.* **16**, 1624 (2005)
4. A.M.A. Al-Kadasi, G.M. Nazeruddin, *J. Chem. Pharm. Res.* **5**, 204 (2013)
5. M.M. Heravi, M. Zakeri, *Synth. React. Inorg. Metal Org. Nano-Met. Chem.* **43**, 211 (2013)
6. M. Kidwai, S. Saxena, R. Mohan, *Synth. Commun.* **42**, 52 (2006)
7. B. Thirupathiah, M. Veerananayana Reddy, Y.T. Jeong, *Tetrahedron* **71**, 2168 (2015)
8. S. Sadjadi, M.M. Heravi, *Curr. Org. Chem.* **20**, 1404 (2016)
9. X. Cuixia, Y. Kedi, L. Zili, Q. Zuzeng, H. Wei, D. Qianwen, Z. Jianjie, Z. Fan, *Chin. J. Chem. Eng.* **22**, 305 (2014)
10. A. Hafizi, A. Ahmadpour, M.M. Heravi, F.F. Bamoharram, *Pet. Sci. Technol.* **32**, 1022 (2014)
11. M.M. Heravi, S. Sadjadi, *J. Iran. Chem. Soc.* **6**, 1 (2009)
12. T. Fotiou, T.M. Triantis, T. Kaloudis, E. Papaconstantinou, A. Hiskia, *J. Photochem. Photobiol. A* **286**, 1 (2014)
13. L. Hong, Y. Gui, J. Lu, J. Hu, J. Yuan, L. Niu, *Int. J. Hydrog. Energy* **38**, 11074 (2013)
14. B.A. Dar, A.K. Sahu, P. Patidar, P.R. Sharma, N. Mupparapu, D. Vyas, S. Maity, M. Sharma, B. Singh, *J. Ind. Eng. Chem.* **19**, 407 (2013)
15. G.D. Yadav, S.O. Katole, A.K. Dalai, *Appl. Catal. A* **477**, 18 (2014)
16. P. Yuan, A. Thill, F. Bergaya (eds.), *Developments in Clay Science*, vol. 7 (Elsevier, 2016), p. iv
17. B. Szczepanik, P. Słomkiewicz, *Appl. Clay Sci.* **124–125**, 31 (2016)
18. S. Barrientos-Ramírez, E.V. Ramos-Fernández, J. Silvestre-Albero, A. Sepúlveda-Escribano, M.M. Pastor-Blas, A. González-Montiel, *Microporous Mesoporous Mater.* **120**, 132 (2009)
19. S. Sadjadi, M.M. Heravi, M. Daraie, *Res. Chem. Intermed.* **43**, 843 (2017)
20. Y. Zhang, A. Tang, H. Yang, J. Ouyang, *Appl. Clay Sci.* **119**, 8 (2016)
21. D. Grabka, M. Raczynska-Žak, K. Czech, P.M. Słomkiewicz, M.A. Józwiak, *Appl. Clay Sci.* **114**, 321 (2015)
22. R.S. Murali, M. Padaki, T. Matsuura, M.S. Abdullah, A.F. Ismail, *Sep. Purif. Technol.* **132**, 187 (2014)
23. M. Massaro, V. Schembri, V. Campisciano, G. Cavallaro, G. Lazzara, S. Milioto, R. Noto, F. Parisi, S. Riela, *RSC Adv.* **6**, 55312 (2016)
24. Y. Zhang, H. Yang, *Phys. Chem. Miner.* **39**, 789 (2012)
25. Y. Zhang, J. Ouyang, H. Yang, *Appl. Clay Sci.* **95**, 252 (2014)
26. M.M. Heravi, E. Hashemi, Y. Shirazi Beheshtiha, S. Ahmadi, T. Hosseinnejad, *J. Mol. Catal. A.* **394**, 74 (2014)
27. M.M. Heravi, F. Mousavizadeh, N. Ghobadi, M. Tajbakhsh, *Tetrahedron Lett.* **55**, 1226 (2014)
28. M.M. Heravi, M. Saeedi, Y.S. Beheshtiha, H.A. Oskooie, *Mol. Divers.* **15**, 239 (2011)
29. S. Sadjadi, M.M. Heravi, M. Daraie, *J. Mol. Liq.* **231**, 98 (2017)
30. S. Sadjadi, M. Eskandari, *Ultrason. Sonochem.* **20**, 640 (2013)
31. M.M. Heravi, S. Sadjadi, N.M. Haj, H.A. Skoobie, F.F. Bamoharram, *Catal. Commun.* **10**, 1643 (2009)
32. M.M. Heravi, S. Sadjadi, H.A. Oskooie, R.H. Shoar, F.F. Bamoharram, *Tetrahedron Lett.* **50**, 662 (2009)
33. Y. Zhang, X. He, J. Ouyang, H. Yang, *Sci. Rep.* **15**, 2948 (2013)
34. S. Mallik, S.S. Dash, K.M. Parida, B.K. Mohapatra, *J. Colloid Interface Sci.* **300**, 237 (2006)

35. S. Sadjadi, M.M. Heravi, M. Daraie, *Res. Chem. Intermed.* **43**, 2201 (2017)
36. H. Zhu, M.L. Du, M.L. Zou, C.S. Xu, Y.Q. Fu, *Dalton Trans.* **41**, 10465 (2012)
37. P. Yuan, P.D. Southon, Z. Liu, M.E.R. Green, J.M. Hook, S.J. Antill, C.J. Kepert, *J. Phys. Chem. C* **112**, 15742 (2008)
38. S. Bordepong, D. Bhongsuwan, T. Punggrassami, T. Bhongsuwan, *J. Sci. Technol.* **33**, 599 (2011)
39. L. Zatta, J.E.F. da Costa Gardolinski, F. Wypych, *Appl. Clay Sci.* **51**, 165 (2011)
40. M. Kidwai, P. Sapra, *Synth. Commun.* **32**, 1639 (2002)
41. H.R. Tavakoli, S.M. Moosavi, A. Bazgir, *J. Korean Chem. Soc.* **57**, 260 (2013)
42. K. Niknam, N. Borazjani, *Monatsh. Chem.* **147**, 1129 (2016)